

# 1 **Genomic sequence characteristics and the empiric 2 accuracy of short-read sequencing**

3  
4 Maximillian Marin<sup>1,2\*</sup>, Roger Vargas Jr<sup>1,2</sup>, Michael Harris<sup>3</sup>, Brendan Jeffrey<sup>3</sup>, L. Elaine  
5 Epperson<sup>4</sup>, David Durbin<sup>5</sup>, Michael Strong<sup>4</sup>, Max Salfinger<sup>6</sup>, Zamin Iqbal<sup>7</sup>, Irada  
6 Akhundova<sup>8</sup>, Sergo Vashakidze<sup>9,10</sup>, Valeriu Crudu<sup>11</sup>, Alex Rosenthal<sup>3</sup>, and Maha Reda  
7 Farhat<sup>1,12\*</sup>

8  
9 1 Department of Biomedical Informatics, Harvard Medical School, Boston, USA

10 2 Department of Systems Biology, Harvard Medical School, Boston, USA

11 3 Office of Cyber Infrastructure and Computational Biology, National Institute of Allergy and Infectious Diseases,  
12 National Institutes of Health, USA

13 4 Center for Genes, Environment, and Health, National Jewish Health, Denver, Colorado, USA

14 5 Mycobacteriology Reference Laboratory, Advanced Diagnostic Laboratories, National Jewish Health, Denver,  
15 Colorado, USA

16 6 College of Public Health & Morsani College of Medicine, University of South Florida, USA

17 7 EMBL-EBI, Wellcome Genome Campus, Hinxton, UK

18 8 Scientific Research Institute of Lung Diseases, Ministry of Health, Baku, Azerbaijan

19 9 The University of Georgia, Tbilisi, Georgia

20 10 National Center for Tuberculosis and Lung Diseases, Ministry of Health, Tbilisi, Georgia

21 11 Phthisiopneumology Institute, Chisinau, Moldova

22 12 Pulmonary and Critical Care Medicine, Massachusetts General Hospital, Boston, USA

23 \*Corresponding authors: mgmarin@g.harvard.edu, Maha\_Farhat@hms.harvard.edu

24

25

26

27

28

29

30

31

32

33

34

35

36

37

38

39

40

41

## 42 **Abstract**

43 **Background:** Short-read whole genome sequencing (WGS) is a vital tool for clinical applications  
44 and basic research. Genetic divergence from the reference genome, repetitive sequences, and  
45 sequencing bias, reduce the performance of variant calling using short-read alignment, but the  
46 loss in recall and specificity has not been adequately characterized. For the clonal pathogen  
47 *Mycobacterium tuberculosis* (Mtb), researchers frequently exclude 10.7% of the genome believed  
48 to be repetitive and prone to erroneous variant calls. To benchmark short-read variant calling, we  
49 used 36 diverse clinical Mtb isolates dually sequenced with Illumina short-reads and PacBio long-  
50 reads. We systematically study the short-read variant calling accuracy and the influence of  
51 sequence uniqueness, reference bias, and GC content. å

52 **Results:** Reference based Illumina variant calling had a recall  $\geq 89.0\%$  and precision  $\geq 98.5\%$  across  
53 parameters evaluated. The best balance between precision and recall was achieved by tuning the  
54 mapping quality (MQ) threshold, i.e. confidence of the read mapping (recall 85.8%, precision  
55 99.1% at  $\text{MQ} \geq 40$ ). Masking repetitive sequence content is an alternative conservative approach  
56 to variant calling that maintains high precision (recall 70.2%, precision 99.6% at  $\text{MQ} \geq 40$ ). Of the  
57 genomic positions typically excluded for Mtb, 68% are accurately called using Illumina WGS  
58 including 52 of the 168 PE/PPE genes (34.5%). We present a refined list of low confidence regions  
59 and examine the largest sources of variant calling error.

60 **Conclusions:** Our improved approach to variant calling has broad implications for the use of WGS  
61 in the study of Mtb biology, inference of transmission in public health surveillance systems, and  
62 more generally for WGS applications in other organisms.

63

## 64 **Background**

65 Illumina short-read whole genome sequencing (WGS) followed by alignment to a reference  
66 genome is widely used to identify genetic variants. Illumina sequencing and alignment can  
67 confidently detect single nucleotide substitutions (SNSs) and small insertions or deletions (INDELS)  
68 but is limited in several ways by its short  $\sim 100$  bp target read lengths. First, short repetitive or  
69 homologous query sequences are challenging to uniquely align to the genomic reference<sup>1,2</sup>. Second,  
70 genomic DNA extraction and sequencing library preparation of short-reads may be more  
71 error or bias prone<sup>3-7</sup>. For example, regions with high GC content and/or low sequence complexity  
72 may be particularly prone to PCR-dropout and reduced sequencing coverage<sup>7-9</sup>. Third, the use of  
73 a single reference genome introduces bias, especially when the genome being analyzed differs  
74 substantially from the reference sequence<sup>10,11</sup>. As the sequenced genome diverges from the  
75 reference genome, short-read alignment becomes increasingly inaccurate and regions absent  
76 from the reference genome are missed or poorly reconstructed.

77

78 In contrast, long-read sequencing can generate high confidence complete genome assemblies,  
79 which can also be used to benchmark Illumina WGS. For example, long-reads generated by PacBio  
80 sequencing (with lengths on the order of ~10 kb) are ideal for assembling complete bacterial  
81 genomes and identifying variants in repetitive regions<sup>12</sup>. Although individual PacBio reads have a  
82 considerably higher per base error rate (10-15%) than Illumina, the randomly distributed nature  
83 of the errors allows for high coverage sequencing runs to converge to a high accuracy consensus<sup>13</sup>.  
84 More recently, circular consensus sequencing has further improved PacBio long-read per base  
85 accuracy to levels on par with Illumina<sup>14</sup>. Alternatively, hybrid strategies that combine less accurate  
86 long-reads and short Illumina reads can offer both high base-level accuracy and continuity of the  
87 final assembly<sup>12,15</sup>.

88

89 *Mycobacterium tuberculosis* (Mtb) is a globally prevalent pathogenic bacterium with a ~4.4 Mbp  
90 genome known for high GC content, large repetitive regions, and an overall low mutation rate.  
91 Owing to the clonality and stability of the Mtb genome, this organism is particularly well suited  
92 for systematically identifying the sources of error that arise when short-read data is used for  
93 variant detection. Approximately 10% of the Mtb reference genome (H37Rv) is regularly excluded  
94 from genomic analysis because it is purported to be more error prone and enriched for repetitive  
95 sequence content<sup>16</sup>. This 10% of the Mtb genome, hitherto regions of putative low confidence  
96 (PLC), span the following genes/families: 1) PE/PPE genes (N=168), 2) mobile genetic elements  
97 (MGEs) (N=147), and 3) 69 additional genes with identified homology elsewhere in the genome<sup>17</sup>.  
98 Despite their systematic exclusion from most Mtb genomic analyses<sup>17-19</sup>, PLC regions are yet to  
99 be evaluated systematically for short-read variant calling accuracy. Here, we use long-read  
100 sequencing data from 36 phylogenetically diverse Mtb isolates to benchmark short-read variant  
101 detection accuracy and study genome characteristics that associate with erroneous variant calls.

102

## 103 **Results**

### 104 **High confidence Mtb assemblies with hybrid short- and long-read sequencing**

105 For this study, PacBio long-read and Illumina sequencing was performed for 31 clinical Mtb  
106 isolates. The resultant data was combined with publicly available paired PacBio and Illumina  
107 genome sequencing of 18 Mtb isolates from two previously published studies<sup>20,21</sup>. From these  
108 datasets, a total of 38 clinical isolates were selected for having a) paired end Illumina WGS with  
109 median sequencing depth  $\geq 40X$  relative to the Mtb reference genome, and b) no evidence of  
110 mixed infections or sample swaps (**Additional File 2**).

111

112 Across these 38 isolates, the mean sequencing depth relative to the H37Rv reference genome was  
113 84x (IQR: 67x - 107x) for Illumina and 286x (IQR: 180x - 367x) for PacBio. We performed *de novo*  
114 genome assembly and iteratively polished each assembly with the PacBio and Illumina reads

115 generating a complete circular assembly for 36/38 isolates (**Methods**). For uniformity in assembly  
116 completeness, we excluded the 2 non-circular assemblies from downstream analysis.  
117

118 We assessed the accuracy of the *de novo* PacBio assemblies by examining the profile of errors  
119 corrected during the Illumina polishing step (**Supp. Figure 1, Additional File 3**). Across all 36  
120 assemblies, erroneous 1-bp insertions and deletions (INDELs) made up 97.9% of all corrections  
121 made by Illumina polishing with Pilon<sup>22</sup>. The median number of erroneous insertions and deletions  
122 per assembly was 5 (IQR: 2 - 88) and 15 (IQR: 4 - 37) respectively. Very few of the errors corrected  
123 during Illumina polishing were single nucleotide changes; median of 0 (IQR: 0 - 2) across all  
124 polished 36 genome assemblies. Overall, the number of changes made during Illumina polishing  
125 of the *de novo* PacBio assembly was negatively correlated to PacBio sequencing depth  
126 (Spearman's R = -0.458, p < 4.9e-3) (**Supp. Figure 1C**).  
127

128 The 36 assemblies spanned the Mtb global phylogeny and had a high degree of conservation in  
129 genome structure and content relative to the H37Rv reference genome (**Figure 1, Supp. Figure**  
130 **2**): Average Nucleotide Identity (ANI) to H37Rv (99.84% to 99.95%), genome size (4.38-4.44 Mb),  
131 GC content (65.59 - 65.64%), and predicted gene count (4017 - 4096 ORFs) (**Additional File 2**).  
132

133 In accordance with the small variant benchmarking guidelines of Global Alliance for Genomics &  
134 Health<sup>23</sup> (GA4GH), we excluded a small subset of regions with ambiguous ground truths on a per  
135 isolate basis (**Methods**). These ambiguous regions fell into 2 categories: a) variable copy number  
136 relative to the H37Rv reference genome or b) difficult to align regions due to a high level of  
137 sequence divergence relative to the reference genome. We excluded these regions from our  
138 performance evaluation in this paper due to their difficulty of interpretation (**Additional File 4**).  
139 The percentage of the genome identified as ambiguous was consistently lower than 1% (median:  
140 0.41%, IQR: 0.28% - 0.49%) across all assemblies. We observed that for the regions that were  
141 frequently ambiguously (Ambiguous in > 25% of isolates, **Additional File 5**), 96.8% of bases were  
142 from regions which overlapped with recognized PLC regions.  
143

#### 144 **Empirical base-level performance of Illumina**

145 To measure the consistency and accuracy of Illumina genotyping across the Mtb genome, we  
146 defined the Empirical Base-level Recall metric (EBR) for each position of the H37Rv reference  
147 genome (4.4 Mb, **Additional File 6**). EBR was calculated as the proportion of isolates for which  
148 Illumina variant calling made a *confident* variant call that agreed with the ground truth, hence a  
149 site with a perfect (1.0) EBR score requires Illumina read data to pass the default quality criteria  
150 (**Methods**), and then agree with the PacBio defined ground truth for 100% of the isolates  
151 (Examples in **Figure 2**). EBR was significantly lower within PLC regions (mean EBR = 0.905, N =  
152 469,501 bp) than the rest of the genome (mean EBR = 0.998, N = 3,942,031 bp, Mann-Whitney

153 U Test,  $P < 2.225\text{e-}308$ ) (**Figure 3A, Table S1**). But EBR was not consistently low across PLC  
154 regions, with 67% of PLC base positions having  $\text{EBR} \geq 0.97$ . EBR averaged by gene (gene-level  
155 EBR) also showed heterogeneity across PLC regions with 62.6%, 61.3% and 82.6% respectively of  
156 the MGEs, PE/PPE, and previously classified repetitive genes having gene-level EBR  $\geq 0.97$  (**Figure**  
157 **3B, Supp. Figure 3, Tables S2-S3, Additional File 7**). All other, non-PLC, functional gene  
158 categories had a median gene-level\_EBR=1, among these only 14 non-PLC genes had a gene-  
159 level EBR  $< 0.97$ .  
160

## 161 **Characteristics of regions with low empirical performance**

162 Across all 36 isolates evaluated, we observed 1,825,385 sites where Illumina failed to confidently  
163 agree with the inferred ground truth. These low recall sites were spread across 267,471 unique  
164 positions of the H37Rv reference genome with  $\text{EBR} < 1$ . We explored the underlying factors  
165 associated with low recall at these positions using the associated filter and quality tags provided  
166 by the variant caller, Pilon (**Methods, Table S4**). Across the 1,829,181 low recall sites, the  
167 distribution of outcomes included: a) 62.78% low coverage (LowCov), b) 30.74% falsely called as  
168 deleted (Del) with or without low coverage or other tags, c) 6.24% were missed deletions tagged  
169 as PASS, d) 0.03% (669 sites) were false base calls (reference or alternate) tagged as PASS, e) 0.25%  
170 remaining positions were labeled as ambiguous (Amb) due to evidence for two or more alleles at  
171 a frequency  $\geq 25\%$ .  
172

173 Among all low recall sites annotated as with a Low Coverage tag: (a) 45.8% were due to insufficient  
174 total coverage of aligned reads (sequencing bias or extreme sequence divergence, total Depth  $<$   
175 5), (b) 27.6% lacked uniquely aligning reads (repetitive sequence content, mapping quality = 0),  
176 and (c) 26.6% were due to low confidence paired-end alignments that did not pass Pilon's  
177 heuristics (likely structural variation causing improper paired-alignment orientation).  
178

## 179 **Repetitive sequence content**

180 We identified repetitive regions in H37Rv and evaluated their relationship with low EBR using the  
181 pileup mappability metric (**Methods**). Pileup mappability scores range from 0 to 1, where 1  
182 represents a genomic position where all overlapping sequence K-mers are unique in the genome  
183 of interest within a similarity threshold of E mismatches. We calculated pileup mappability  
184 conservatively with a K-mer size of 50 base pairs and up to 4 mismatches (P-Map-K50E4,  
185 **Additional File 6**). P-Map-K50E4 is lower in PLC regions (mean = 0.856) than non-PLC regions  
186 (mean = .997), (Mann-Whitney U Test,  $P < 0.001$ ) (**Figure 3A**). Yet, 69.7% of positions in PLC  
187 regions had P-Map-K50E4 scores of 1, indicating uniquely alignable sequence content even with  
188 sequence lengths as short as 50 bp (**Table S5**). At the gene-level, PE/PPEs and MGEs had lower P-  
189 Map-K50E4 than the rest of the genome (Wilcoxon,  $P < 2\text{e-}308$ ) (**Figure 3B, Table S6, Additional**  
190 **File 7**) but 34.5%, and 32.7% of these genes respectively had perfect (1.0) P-Map-K50E4 across

191 the entire gene body. Previously identified repetitive genes (N = 69) had a gene-level P-Map-K50  
192 below 1 which is expected given that this was their defining feature<sup>24</sup>, but for the majority (51 of  
193 69), median mappability was greater than 0.99, indicating that a high proportion of their sequence  
194 content was actually unique. Non-PLC functional categories had a median gene level P-Map-  
195 K50E4 = 1.0 (**Supp. Figure 3, Table S7**). Genome-wide P-Map-K50E4 and EBR scores were  
196 moderately correlated (Spearman's  $\rho$ = 0.47,  $P < 2e-308$ ). Thirty percent of all genome positions  
197 with EBR < 1.0 also had a P-Map-K50E4 score below 1.0.

198

### 199 **Sequencing bias in high GC-content regions**

200 Across several sequencing platforms, high-GC content associates with low sequencing depth due  
201 to low sequence complexity, PCR biases in the library preparation and sequencing chemistry<sup>3-6</sup>.  
202 We assessed the sequencing bias of Illumina and PacBio across each individual genome assembly  
203 using the relative depth metric<sup>4</sup> (the depth per site divided by average depth across the entire  
204 assembly) to control for varying depth between isolates. On average with Illumina, 1.2% of the  
205 genome had low relative depth (< 0.25), while for PacBio sequencing the average proportion of  
206 the genome with low relative depth was 0.0058% (Mann-Whitney U Test,  $P < 0.001$ ). Both  
207 sequencing technologies demonstrated coverage bias against high-GC regions, with more  
208 extreme bias for Illumina than PacBio (**Figure 4, Additional File 8**). Across all base pair positions  
209 with local GC%  $\geq$  80%, using a window size of 100 bp, the mean relative depth was 0.79 for PacBio  
210 and 0.35 for Illumina. Genome-wide, EBR was significantly negatively correlated with GC content  
211 (Spearman's  $\rho$ = - 0.12,  $P < 2e-308$ ), but this correlation was weaker than that observed with  
212 sequence uniqueness (P-Map-K50E4, as above Spearman's  $\rho$ =0.47).

213

### 214 **False positive SNS variant calls**

215 Next, we focused specifically on regions with high numbers of false positive SNSs identified  
216 through comparison with the ground-truth variant calls. We examined the distribution of false  
217 positive SNS calls across the H37Rv reference genome using a realistic intermediate variant  
218 filtering threshold of mean mapping quality at the variant site (MQ  $\geq$  30, **Figure 5, Additional**  
219 **File 9**). The top 30 regions ranked by the number of false positives (23 genes and 7 intergenic  
220 regions) contained 89.4% (490/548) of the total false positive calls and spanned 65 kb, 1.5% of the  
221 H37Rv genome. Of these 30 false positive hotspot regions, 29 were either a PLC gene or an  
222 intergenic region adjacent to a PLC gene: 17 PE/PPE genes, 3 MGEs, 2 were previously identified  
223 repetitive genes<sup>24</sup>, and 7 PLC-adjacent intergenic regions. Across all false positives, the PE-PGRS  
224 and PPE-MPTR sub-families of the PE/PPE genes were responsible for a large proportion (45.4%)  
225 of total false positive variant calls. Of all the 556 false positives SNSs evaluated (MQ  $\geq$  30), only  
226 14 were detected across 4 non-PLC genes: Rv3785 (9 FPs), Rv2823c (1 FP), plsB2 (2 FPs), Rv1435c  
227 (2 FPs).

228

229 **Masking to balance precision and recall**

230 A common approach for reducing *Mtb* false positive variant calls is to mask/exclude all PLC  
231 regions from variant calling. Here we investigated two variations on this that utilize directly  
232 reference sequence uniqueness and variant quality metrics. We compared: (1) masking of regions  
233 with non-unique sequence, defined as positions with P-Map-K50E4 < 1, (2) No *a priori* masking  
234 of any regions, and (3) masking of all PLC genes (the current standard practice). We then filtered  
235 potential variant calls by whether the variant passed all internal heuristics of the Pilon<sup>22</sup>-based  
236 variant calling pipeline (**Methods**) and studied the effect of varying the mean mapping quality  
237 (MQ) filtering threshold from 1 to 60 (**Figure 6**). We computed the F1-score, precision and recall  
238 of detection of SNSs and small indels (<=15bp) for each masking schema and MQ threshold  
239 across all 36 clinical isolates (**Methods, Additional File 10**).

240

241 For SNSs, mean recall ranged from 63.6% to 89.0%, and precision ranged from 98.5% to 99.97%  
242 across the three schemas (**Figure 6A**). At a threshold of MQ  $\geq 40$ , we observed the following mean  
243 SNS performances: 1) Masking non-unique regions, F1 = 0.87 (Precision = 99.8%, Recall = 77.9%),  
244 2) no masking of the genome, F1 = 0.92 (Precision = 99.1%, Recall = 85.8%), 3) Masking PLC  
245 genes, F1 = 0.82 (Precision = 99.6%, Recall = 70.2%). Based on F1 score, no masking of the genome  
246 had the highest overall performance, but masking non-unique regions had the highest precision.  
247 Decreasing the MQ threshold to an optimal value for F1 score resulted in similar performance for  
248 schema-1 and 3, but a balance of lower precision and higher recall for schema-2. Increasing the  
249 MQ threshold to 60 optimized precision but at considerable loss of recall for all three schemas  
250 (**Table 1**). Performance was most sensitive to the MQ threshold under schema 2 (no masking).

251

252 For INDELs (1-15 bp), precision was comparable to SNSs (96.2% - 100%, **Figure 6B**), while recall  
253 was lower (48.9% - 82.4%). At a threshold of MQ  $\geq 40$ , we observed the following mean INDEL  
254 performances: 1) Masking non-unique regions, F1 = 0.83 (Precision = 98.2, Recall = 72.1%), 2) no  
255 masking of the genome, F1 = 0.89 (Precision = 98.9, Recall = 80.8%), 3) Masking PLC genes, F1 =  
256 0.76 (Precision = 99.1%, Recall = 61.5%). Variant calling performance of short (1-5bp) INDELs was  
257 comparable to SNSs, and the limited performance for INDELs was largely driven by low recall of  
258 longer (6-15bp) INDELs (**Supp. Figure 5, Additional File 11**).

259

260 **Structural variation**

261 We assessed the effect of structural variation (SV), of length  $\geq 50$  bp, a common source of  
262 reference bias, on variant calling performance (**Methods**). Detected SVs included the known  
263 regions of difference associated with *Mtb* Lineages 1, 2 and 3 (RD239, RD181, RD750  
264 respectively)<sup>25,26</sup> (**Supp. Figure 6**). Across all 36 isolate assemblies, we observed a strong negative  
265 correlation between average nucleotide identity to the H37Rv reference and the number of SVs

266 detected (Spearman's R = -0.899, p < 1.1e-13, **Supp. Figure 7**). Additionally, we observe that 70%  
267 of detected SVs overlapped with regions with low pileup mappability (P-Map-K50E4 < 1.0).  
268

269 We compared SNS variant calling performance by proximity to an SV and sequence uniqueness  
270 (**Figure 7, Additional File 12**), dividing variants into four groups: (1) SNSs in regions with perfect  
271 mappability (Pmap-K50E4 = 1) with no identified SV (87.3% of total 47,412 SNSs), (2) SNSs in  
272 regions with low mappability (Pmap-K50E4 < 1) with no identified SV (10.9% of SNSs), (3) SNSs in  
273 regions with perfect mappability within 100 bp of any identified SV (0.8% of SNSs), and (4) SNSs  
274 in regions with low mappability within 100bp of any identified SV (1.0% of SNSs). Variant calling  
275 performance decreased most sharply in regions with evidence for structural variation, especially  
276 when sequence content is also non-unique (Region types 3 & 4 respectively). Additionally, region  
277 type (2), or low mappability sequence content with no nearby SV, demonstrated reduced  
278 performance.  
279

## 280 **Refined regions of low confidence**

281 Based on the presented analysis, we define a set of refined low confidence (RLC) regions of the  
282 Mtb reference genome. The RLC regions are defined to account for the largest sources of error  
283 and uncertainty in analysis of Illumina WGS, and is defined as the union of A) The 30 false positive  
284 hot spot regions identified (65 kb), B) low recall genomic regions with EBR < 0.9 (142 kb with 30  
285 kb overlap with (A)), and C) regions ambiguously defined by long-read sequencing (**Methods**, 16  
286 kb). We additionally evaluated the overlap between all detected SVs and the three RLC categories:  
287 RLC subset (A) overlapped 28% of SVs, RLC subset (B) overlapped with 65% of SVs, RLC subset (C)  
288 overlapped with 14% of SVs.  
289

290 In total, the proposed RLC regions account for 177 kb (4.0%) of the total H37Rv genome  
291 (**Additional File 13**) and their masking represents a conservative approach to variant filtering.  
292 Across the 36 isolates evaluated, masking of the RLC regions combined with a SNS filter of MQ  $\geq$   
293 40 would produce a mean F1-score of 0.882, with a mean precision of 99.9% and a mean recall of  
294 78.9%.  
295

## 296 **Discussion**

297 The analysis and interpretation of Illumina WGS is critical for both research and clinical  
298 applications. Here, we study the 'blindspots' of paired-end Illumina WGS by benchmarking  
299 reference-based variant calling accuracy using 36 Mtb isolates with high confidence complete  
300 genome assemblies. Overall, our results improve our general understanding of the factors that  
301 affect Illumina WGS performance. In particular, we systematically quantify variant calling accuracy  
302 and the effect of sequence uniqueness, GC-content, coverage bias, and structural variation. For  
303 Mtb, we demonstrate that a much greater proportion of the genome can be analyzed with Illumina

304 WGS than previously thought and provide a systematically defined set of low  
305 confidence/troublesome regions for future studies.

306  
307 Approaches to benchmarking variant calling from Illumina WGS vary by field and species of  
308 interest and more standardization is needed<sup>27</sup>. Variant calling accuracy is usually benchmarked  
309 through *in silico* variant introduction with read simulation or otherwise using a small number of  
310 reference genomes that seldom capture the full range of diversity within a particular species. Our  
311 benchmarking exercise is unique in using a large and diverse set of high quality genome  
312 assemblies that are built using a hybrid long and short read approach. We further demonstrate  
313 that PacBio long-read sequencing is much less prone to coverage bias and is able to generate  
314 complete circular bacterial assemblies bridging repetitive regions in the majority of isolates with  
315 a median depth > 180x. The assemblies we generate will be an important community resource for  
316 benchmarking future variant calling or other WGS based bioinformatics tools.

317  
318 The benchmarking results clearly demonstrate that low variant recall is a major limitation of  
319 reference-based Illumina variant calling, which achieved at most 89% recall at the optimal F1-  
320 score. Precision of variant calling using Illumina on the other hand was very high, with the small  
321 number of false variant calls concentrated in repetitive and structurally variable regions. We find  
322 that the best balance between precision and recall is achieved by tuning the variant mean  
323 mapping quality threshold, i.e. confidence of the read mapping. The specific mapping quality  
324 threshold will likely vary by species. For a GC-rich organism with highly repetitive sequence  
325 content like Mtb, a threshold of 40 achieved 85.8% recall and 99.1% precision.

326  
327 Studying specific sources of low recall from Illumina, we identified insufficient read coverage to  
328 be the major driver, due not only to repetitive sequence content but also due to high-GC content  
329 and other sources of coverage bias. We further identified regions near structural variation to be  
330 particularly prone to low recall and precision. Of the variants we study, longer INDELS were recalled  
331 at lower rates than SNSs or INDELS < 6bp in length. These observations support ongoing efforts  
332 by the bioinformatics research community to build graph-reference genomes and align short  
333 reads to these graphs. Using a graph pan-genome built with a diverse set of Mtb reference  
334 genomes, there is great potential to both increase recall and precision of variant calling in  
335 divergent regions of the genome.

336  
337 An alternative and generalizable approach to balancing precision and recall of reference-based  
338 Illumina variant calling is to mask repetitive (low mappability) regions. This simple approach does  
339 not require tuning the mapping quality threshold against a ground truth set of assemblies and  
340 relies instead on computing the pileup mappability metric across the reference sequence. This fills  
341 a gap for variant calling in other organisms using short-read mapping where low confidence  
342 regions may not already be defined. Compared with tuning against a ground-truth set of

343 assemblies, this masking approach is conservative: for Mtb and filtering by MQ  $\geq 40$ , precision is  
344 slightly higher at 99.8% vs 99.1% respectively and recall is lower at 77.9% vs 85.8% respectively.  
345

346 Given Mtb's genomic stability and clonality, this organism is particularly well suited for  
347 systematically identifying the sources of variant calling error from short-read data. Although  
348 10.7% of the Mtb reference sequence is commonly excluded from genomic analysis, our results  
349 demonstrate that more than half of these regions are accurately called using Illumina WGS. For  
350 the PE/PPE family, of highest concern for sequencing error, nearly one third (52/168) had perfect  
351 mappability and near perfect gene-level EBR ( $\geq 0.99$ ). The PE/PPE genes with poor performance  
352 were largely the PE\_PGRS and PPE\_MPTR sub-families. Only 65 kb (1.5%) of the reference genome  
353 H37Rv were responsible for the majority of false positives (89.2% of false positives across 36  
354 isolates).

355  
356 We present a set of refined low confidence (RLC) regions of the Mtb genome, designed to account  
357 for the largest sources of error and uncertainty in analysis of Illumina WGS (**Additional File 13**).  
358 Long-read data can allow RLC regions to be defined for other species to improve accuracy of  
359 Illumina WGS. The Mtb RLC regions span 4.0% of the reference genome, and their masking  
360 provides a conservative approach to variant calling, appropriate for applications where precision  
361 is prioritized over recall. At the same time, RLC region masking offers higher recall than the current  
362 field standard where more than 10% of the Mtb reference genome is masked. One limitation is  
363 that RLC regions were largely defined based on EBR of Illumina sequencing in our dataset that  
364 was restricted by design to 100+ bp paired end sequencing. We do not recommend the use of  
365 these RLC regions for Illumina sequencing at shorter read lengths or single-end reads. Instead we  
366 make available a more appropriate masking scheme of RLC regions + low pileup mappability  
367 (**Additional File 14**). Another limitation is that we defined RLC regions using the same set of high  
368 confidence assemblies evaluated. The reported precision and recall with RLC region masking are  
369 thus likely overestimates. On the other hand, we expect precision and recall estimates of the  
370 alternative approaches of masking low mappability regions or filtering at MQ  $\geq 40$  to be more  
371 robust.

372  
373 Improving Illumina variant recall has significant implications. For clonal Mtb, for example,  
374 transmission inference using genomic data often relies on a very small number of SNS or INDEL  
375 differences between genome pairs. The observed large increase in recall we observe has the  
376 potential to substantially improve transmission inference<sup>28</sup> and/or our understanding of genome  
377 stability and adaptation.

378

## 379 **Conclusions**

380 In summary, we show that Illumina whole genome sequencing has high precision but limited recall  
381 in repetitive and structurally variable regions when benchmarked against a diverse set of complete  
382 assemblies. We demonstrate that filtering variants using the mean mapping quality against a  
383 achieves the highest balance of precision and recall. Masking repetitive sequence content is a  
384 second generalizable solution, albeit a more conservative one, that maintains high precision. For  
385 *Mtb*, these two approaches increase recall of variants by 15.6% and 7.7% respectively, with a  
386 minimal change in precision (-0.5% and +0.1% respectively at  $\text{MQ} \geq 40$ ), allowing high variant  
387 recall in >50% of regions previously considered by the field to be error-prone. Our results improve  
388 variant recall from Illumina data with broad implications for clinical and research applications of  
389 sequencing. We also provide a high-quality set of genome assemblies for benchmarking future  
390 variant calling or other WGS based bioinformatics tools.

## 391 **Methods**

### 392 **Summary of sequencing data used**

393 Our dataset consisted of a convenience set of 16 clinical isolates from Lima, Peru, previously  
394 sequenced with Illumina WGS and archived in frozen culture<sup>29</sup>. These isolates were revived and  
395 sequenced with PacBio RS II long-read sequencing (Dataset #1). Additionally, 15 total clinical  
396 isolates isolated in Azerbaijan, Georgia, Moldova were sequenced with PacBio Sequel II long-read  
397 sequencing<sup>30</sup> (Dataset #2).

398

399 This dataset of 31 clinical isolates was combined with publicly available paired PacBio (RS II) and  
400 Illumina genome sequencing from 19 clinical isolates from two previously published studies<sup>20,21</sup>.  
401 From these four sources, 38 Mtb isolates were selected for having a) Illumina WGS with paired  
402 end reads with at least a median sequencing depth of 40X relative to the Mtb reference genome  
403 (H37Rv). All aggregated metadata and SRA/ENA accessions for PacBio and Illumina sequencing  
404 data associated with this analysis can be found in **Additional File 15**.

405

### 406 **DNA extraction for PacBio (RS II) Sequencing of Peruvian Isolates (Data Source #1)**

407 MTB cultures were allowed to grow for 4-6 weeks. Pellets were heat-killed at 80°C for 20  
408 minutes<sup>67,68</sup>, the supernatants were removed, and the enriched cell pellet was subjected to DNA  
409 extraction soon after or stored frozen until extraction. Largely intact DNA was extracted from heat-  
410 killed cells pellets using a protocol tailored for mycobacteria that ends with a column-based  
411 elution<sup>31</sup>. Yields were determined using fluorescent quantitation (Qubit, Invitrogen/Thermo Fisher  
412 Scientific) and quality was assessed on a 0.8% GelRed agarose gel with 1XTAE, separated for 90  
413 minutes at 80V.

414

### 415 **PacBio (RS II) Sequencing of Peruvian Mtb Isolates (Data Source #1)**

416 Approximately 1 µg of high molecular weight genomic DNA was used as input for SMRTbell  
417 preparation, according to the manufacturer's specifications (SMRTbell Template Preparation Kit  
418 1.0, Pacific Biosciences). Briefly, HMW gDNA was sheared to 20kb using the Covaris g-tube at 4500  
419 rpm. Following shearing, gDNA underwent DNA damage repair, ligation to SMRTbell adaptors  
420 and exonuclease treatment to remove any unligated gDNA. At least 500 ng final SMRTbell library  
421 per sample was cleaned with AMPure PB beads and 3-50 kb fragments were size selected using  
422 the BluePippin system on 0.75% agarose cassettes and S1 ladder, as specified by the manufacturer  
423 (Sage Science). Size selected SMRTbell libraries were annealed to sequencing primer and bound  
424 to the P6 polymerase prior to loading on the RSII sequencing system (Pacific Biosciences).  
425 Sequencing was performed using C4 chemistry and 240-minute movies. Following data collection,  
426 raw data was converted into subreads for subsequent analysis using the RS\_Subreads.1 pipeline  
427 within SMRTPortal (version 2.3), the web-based bioinformatics suite for analysis of RSII data.

428

429 **DNA extraction for PacBio (Sequel II) Sequencing (Data Source #2)**

430 For all samples from Azerbaijan and Georgia, MTB cultures were grown in 7H9+ADST broth to  
431 A600 0.5–1.0. Pelleted cells were heat killed at 80°C for 2 hours. Cell pellets were resuspended in  
432 450ul TE-Glu, 50ul of 10 mg/mL lysozyme was added and incubated at 37°C overnight. To each  
433 sample 100ul of 10% sodium dodecyl sulfate and 50ul of 10 mg/ml proteinase K was added and  
434 incubated at 55°C for 30 minutes. 200 ul of 5M sodium chloride and 160 ul Cetramide Saline  
435 Solution (preheated 65°C) was added then incubated for 65°C for 10 minutes. To each sample 1  
436 ml chloroform:isoamyl alcohol (24:1) was added, mixed gently by inversion. Samples were  
437 centrifuged at 5000g for minutes, and 900ul of aqueous layer was transferred to fresh tube. DNA  
438 was re-extracted with chloroform:isoamyl alcohol (24:1) and 800 ul of aqueous layer was  
439 transferred to fresh tube. To 800 aqueous layer 560 ul isopropanol was added, mix gently by  
440 inversion. The precipitated DNA was collected by centrifuging for 10 minutes and supernatant  
441 was removed. DNA was washed with 70% ethanol, and DNA was collected by centrifuging and  
442 supernatant removed. Air dried DNA pellet was dissolved overnight in 100 ul of TE buffer, and  
443 stored at 4°C.

444

445 For all samples from Moldova, DNA was extracted according to CTAB protocol<sup>32</sup>.

446

447 **PacBio (Sequel II) Sequencing (Data Source #2)**

448 Approximately 1 µg of high molecular weight genomic DNA was used as input for SMRTbell  
449 preparation according to the manufacturer's protocol (Preparing Multiplexed Microbial Libraries  
450 Using SMRTbell Express Template Prep Kit 2.0, Pacific Biosciences). Briefly, HMW gDNA was  
451 sheared to ~15kb using the Covaris g-tube at 2029 x g. For about half of the samples the  
452 molecular weight of the DNA did not need shearing. Following shearing, gDNA underwent DNA  
453 damage repair, ligation to SMRTbell barcoded adaptors and exonuclease treatment to remove  
454 any unligated gDNA. At least 500 ng of pooled SMRTbell library per sample was cleaned with  
455 AMPure PB beads and 7-50 kb fragments were size selected using the BluePippin system on 0.75%  
456 agarose cassettes and S1 ladder, as specified by the manufacturer (Sage Science). The pool of  
457 size-selected SMRTbell libraries were annealed to v4 sequencing primer and bound to the  
458 polymerase prior to loading on the Sequel II sequencing system (Pacific Biosciences). Sequencing  
459 was performed using version 1 chemistry and 15-hour movies.

460

461 **H37Rv reference genome and gene annotations**

462 The H37Rv (NCBI Accession: NC\_000962.3) genome sequence and annotations was used as the  
463 standard reference genome for all analyses. Functional category annotations for all genes of  
464 H37Rv were downloaded from Release 3 (2018-06-05) of MycoBrowser<sup>33</sup>  
465 (<https://mycobrowser.epfl.ch/releases>). PE/PPE sub-family annotations of H37Rv were taken from

466 Ates et al.<sup>34</sup>. Programmatic visualization of data along with annotations of the H37Rv genome  
467 were made using the DNA Features Viewer python library<sup>35</sup>.

468

#### 469 **Genome assembly with PacBio long-read data**

470 All PacBio reads were assembled using Flye<sup>36</sup> (v2.6). After assembly, Flye performed three rounds  
471 of iterative polishing of the genome assembly with the PacBio subreads, producing a polished de  
472 novo PacBio assembly. If Flye identified the presence of a complete circular contig, Circlator<sup>37</sup>  
473 (v1.5.5) was used to standardize the start each assembly at the DnaA (Rv0001) locus.

474

#### 475 **Polishing of *de novo* PacBio assemblies with Illumina WGS**

476 The paired-end Illumina WGS reads were trimmed with Trimmomatic<sup>38</sup> (v0.39) with the following  
477 parameters: 2:30:10:2:true SLIDINGWINDOW:4:20 MINLEN:75. Trimmed reads were aligned to the  
478 associated de novo PacBio assembly with BWA-MEM<sup>39</sup> (v0.7.17). Duplicate reads were removed  
479 from the resulting alignments using PICARD<sup>40</sup> (v2.22.5). Using the deduplicated alignments, Pilon<sup>22</sup>  
480 (v1.23) was then used to correct SNSs and small INDELs in the *de novo* PacBio assembly, producing  
481 a high confidence assembly polished by both PacBio and Illumina WGS.

482

#### 483 **Identifying mixed infections using F2 metric and removing mismatched PacBio and 484 Illumina WGS**

485 To further reduce the effects of contamination, we used the F2 metric to identify samples that  
486 may have inter-lineage variation due to co-infection<sup>41</sup>. The F2 metric measures the heterogeneity  
487 of genotypes at known lineage defining positions of the H37Rv genome. We computed the F2  
488 lineage-mixture metric for both PacBio and Illumina WGS from each isolate. Isolates were filtered  
489 out if either the F2 metric for Illumina sequencing passed 0.05 or the F2 metric for PacBio  
490 sequencing passed 0.35. The threshold used for PacBio sequencing subreads is much higher  
491 because the inherent error rate per read is much higher than Illumina.

492

493 During polishing we identified the N0052 isolate from Chiner-Oms et al.<sup>20</sup> as a potential sample  
494 mismatch, meaning PacBio and Illumina WGS were not performed on the same clinical isolate.  
495 When polishing the *de novo* assembly of N0052, we found that the following changes were  
496 performed based on the Illumina WGS: 594 SNPs, 19 insertions, and 92 deletions. The extreme  
497 number of corrected SNPs by Illumina polishing is drastically different from the known error  
498 profile (**Additional File 2-3**). Additionally, the inferred sub-lineage of the *de novo* PacBio  
499 assembly was lineage 2.2.1, while the inferred sub-lineage based on Illumina WGS and the Illumina  
500 Polished PacBio assembly was lineage 2.2.2 (**Additional File 2**). The fact that the polishing with  
501 Illumina WGS changed known lineage defining SNPs makes the sample further suspect as a  
502 mismatch. Thus, N0052 was removed from analysis as to minimize chances of benchmarking  
503 wrongly matched data.

504

## 505 **Evaluation of PacBio genome assembly characteristics and multiple genome 506 alignment**

507 FastANI<sup>42</sup> was used to calculate the average nucleotide identity to the H37Rv reference genome  
508 for all completed genome assemblies. The Prokka (v1.13) genome annotation pipeline<sup>43</sup> was used  
509 to annotate genes in each completed genome assembly. The genome size and GC content of the  
510 entire genome was calculated from each assembly using custom python code. The  
511 progressiveMauve algorithm of the Mauve (v2.4.0)<sup>44</sup> alignment software was used to perform  
512 multiple sequence alignment of all 36 completed Mtb assemblies and the H37Rv reference  
513 genome (NCBI Accession: NC\_000962.3). The multiple genome alignments of H37Rv and 36  
514 assemblies were visualized using the Mauve GUI<sup>45</sup> (**Supp. Figure 2**).

515

## 516 **Variant calling and structural variant detection using complete PacBio assemblies**

517 Minimap2<sup>46</sup> was used to align each polished circular completed assembly to the H37Rv reference  
518 genome, producing a base-level alignment of similar regions of the assembly to H37Rv. In regions  
519 with high sequence diversity or large structural variation, Minimap2 will not produce alignments.  
520 To account for this, the NucDiff<sup>47</sup> analysis pipeline, which uses the MUMmer<sup>48</sup> aligner internally,  
521 was also used to detect and classify the presence of large structural variants relative to the H37Rv  
522 reference. All structural variants ( $\geq 50$  bp) identified by NucDiff for each genome assembly can be  
523 found in (**Additional File 16**).

524

## 525 **Illumina WGS data processing for variant calling relative to H37Rv**

526 Paired-end Illumina reads were trimmed with Trimmomatic (v0.39) with the following parameters:  
527 2:30:10:2:true SLIDINGWINDOW:4:20 MINLEN:75. Trimmed reads were aligned to the H37Rv  
528 reference genome (NC\_000962.3) with BWA-MEM<sup>39</sup> (v0.7.17). Duplicate reads were removed from  
529 the resulting alignments using PICARD<sup>40</sup> (v2.22.5). Using the deduplicated alignments, small  
530 genome variants (SNSs and INDELs) were inferred using Pilon<sup>22</sup> (v1.23). Samtools, Bcftools, and  
531 BEDtools were used as needed for SAM/BAM, and VCF/BCF format file manipulation<sup>49-51</sup>.

532

## 533 **Phylogenetic inference using complete genome assemblies**

534 All single nucleotide variants inferred through alignment with Minimap2 of PacBio assembly to  
535 the H37Rv genome were concatenated across the 36 strains. Any SNS position which was ever  
536 ambiguously called in at least 1 isolate was excluded (No NAs allowed, only REF or ALT alleles  
537 allowed). Thus, in order for a SNS position to be included it needed to have no ambiguity relative  
538 to the H37Rv reference in any isolate. FastTree<sup>52</sup> was used to infer an approximate maximum  
539 likelihood phylogeny from the concatenated SNS alignment of all 36 clinical Mtb isolates (15,673  
540 total positions across 36 Mtb clinical isolates).

541

542 **Measuring repetitive sequence content of the H37Rv reference genome using Pileup**  
543 **Mappability**

544 We evaluated sequence uniqueness using a *mappability* metric defined as the inverse of the  
545 number of times a sequence of length  $K$  appears in a genome allowing for  $e$  mismatches and  
546 considering the reverse complement<sup>53</sup>. The *pileup mappability* of a position in a genome is then  
547 defined as the average mappability of all overlapping k-mers. Thus, there are 2 parameters when  
548 calculating mappability,  $k$  (length of k-mer) and  $e$  (number of base mismatches allowed in  
549 counting matching k-mers). Genmap<sup>54</sup> (v1.3) was used to calculate the mappability of all k-mers  
550 across the H37Rv reference genome with the following parameters: k-mer sizes of 50, 75, 100,  
551 125, 150 base pairs and  $E = 0-4$  mismatches. The Gene-level mappability ( $k = 50$  bp,  $e = 4$   
552 mismatches) scores were computed as the average pileup mappability across all genes bodies  
553 annotated in H37Rv (NCBI Accession: NC\_000962.3). The base level pileup mappability scores of  
554 H37Rv are available in TSV and BEDGRAPH format for easy visualization in a genome browser  
555 (**Additional Files 6 and 17**).

556

557 **Calculation of Empirical Base-level Recall (EBR) of Illumina variant calling**

558 The goal of the empirical base-level recall (EBR) for score is to summarize the consistency by which  
559 Illumina WGS correctly evaluated any given genomic position. The EBR for a genomic position  
560 was defined as the proportion isolates where Illumina WGS confidently and correctly agreed with  
561 the PacBio defined ground truth. The ground truth was inferred for each isolate by directly  
562 comparing the completed PacBio genome assembly to the H37Rv reference using Minimap2<sup>46</sup>  
563 and NucDiff<sup>47</sup>. Due to Minimap2's inability to classify large structural variants, the ground truth  
564 relative to H37Rv was supplemented with the structural variant calls generated by the NucDiff  
565 analysis pipeline. Illumina WGS reads were aligned to the H37Rv reference genome with BWA-  
566 MEM<sup>39</sup>, and variants were inferred with the Pilon<sup>22</sup> variant detection tool. In addition to identifying  
567 variants relative to the reference genome, Pilon provides variant calling annotations for all  
568 positions of H37Rv. The variant calling quality annotations of Pilon for all positions of H37Rv were  
569 parsed for comparison to the PacBio defined ground truth for each isolate evaluated.

570 Only the following comparison outcomes were classified as a correctly recalled position:

571 1) Both Illumina variant calling and the PacBio ground truth agree on the genotype of a genomic  
572 position, 2) Both Illumina variant calling and the PacBio ground truth agree that a genomic  
573 position is deleted.

574

575 The following comparison outcomes were classified as poorly recalled position:

576 3) The PacBio ground truth supports a deletion, but Illumina is not confident in the presence of  
577 the deletion, 4) Both Illumina variant calling and the PacBio ground truth disagree on the genotype  
578 of a genomic position, 5) The PacBio ground truth supports the presence of a genomic region,  
579 while Illumina variant calling did not confidently support the presence of the region. 6) Illumina

580 variant calling erroneously supports a deletion at a genomic position which is not deleted in the  
581 PacBio ground truth.

582  
583 The following EBR comparison outcomes were classified as ambiguous (N/A) due to ambiguities  
584 in the interpretation of the ground truth: a) Cases where the PacBio ground truth contained  
585 genome duplications relative to H37Rv, b) Cases where the PacBio ground truth did not provide  
586 a confident alignment or structural variant call due to high sequence divergence from the  
587 reference sequence.

588  
589 For calculating the EBR for a genomic position, ambiguous (N/A) outcomes were ignored when  
590 the number of N/As was  $\leq 25\%$ . In the case that a position had greater than 25% N/As at a  
591 genomic position, the EBR score was defined as "Ambiguous". Ambiguous (N/A) EBR scores  
592 represent locations of the H37Rv genome where there appeared to be systematic trouble in  
593 determining the ground truth genotype.

594  
595 The base level EBR scores are available in TSV and BEDGRAPH format for easy visualization in a  
596 genome browser (**Additional Files 6 and 18**).

597  
598 **Evaluating characteristics of low empirical performance across Mtb genome**

599 The Illumina WGS variant caller used, Pilon, produces VCF tags for all reference positions  
600 evaluated, including positions which were confidently called a reference. The tags associated with  
601 each position can either be PASS or a combination of non-pass tags (LowCov, Del, Amb). Each  
602 genomic position can be assigned a combination of the following VCF Tags: a) PASS, signifying  
603 confirmation of either a reference or an alternative allele. b) LowCov, signifying insufficient high  
604 confidence reads (Depth  $< 5$ ). c) Del, signifying that the position is confidently inferred to be  
605 deleted. d) Amb, signifying evidence for more than one allele at this position. We quantified the  
606 frequency of all combinations of these tags across all positions that were classified as "poor  
607 recalled" during EBR evaluation.

608  
609 **Measuring sequencing bias with per-base relative depth**

610 We measured sequencing bias using the relative depth statistic, which for a given genome  
611 assembly and sequencing dataset, is defined as the sequencing depth per site divided by average  
612 depth across the entire genome<sup>4</sup>. We evaluated the relative depth of all base pair positions of all  
613 sequencing runs (Illumina and PacBio) relative to the corresponding isolates' complete PacBio  
614 genome assembly. The sequencing depth of a base pair position was defined as the number of  
615 reads with a nucleotide aligning to the position of interest. We calculated the mean coverage  
616 across a sample by simply averaging the depth across all positions of the evaluated genome. For  
617 ambiguous mapping reads, the aligners used (BWA-mem and Minimap2) use a random

618 assignment policy between all possible alignment locations. This allows for approximation of  
619 depth in regions with non-uniquely mapping reads. For each individual *Mtb* isolate, we then  
620 calculated the mean relative depth across all positions with the same GC content (100 bp window  
621 size, **Additional File 8**).

622

## 623 **Defining and excluding ambiguous regions relative to H37Rv (per isolate genome 624 assembly)**

625 Following GA4GH (Global Alliance for Genomics & Health) benchmarking guidelines<sup>23</sup>, we  
626 excluded regions of the genome, where definition of the ground truth had ambiguity in its  
627 definition relative to the reference genome. The following comparison outcomes were classified  
628 as ambiguous (N/A) due to ambiguities in the interpretation of the ground truth: a) Cases where  
629 the PacBio ground truth contained duplications relative to H37Rv, b) Cases where the PacBio  
630 ground truth did not provide a confident alignment or structural variant call due to high sequence  
631 divergence relative to H37Rv. These regions thus represent sequences of divergence relative to  
632 the reference genome.

633

634 The percentage of the reference genome that was identified as “ambiguous” was consistently less  
635 than 1% for all 36 clinical isolates evaluated. The median percent of the genome where the ground  
636 truth was “ambiguously defined” was 0.4% (IQR: 0.3% - 0.5%). A large majority of these ambiguous  
637 ground truth regions were either in Mobile Genetic Elements, PE\_PGRS or PPE\_MPTR genes. The  
638 ambiguously defined regions for each isolate can be found in **Additional File 4**. Additionally, all  
639 regions of the H37Rv genome which were ambiguous in over 25% of isolates, signifying high  
640 levels of ambiguity, are present in **Additional File 5**.

641

## 642 **Defining the putative low confidence (PLC) regions of the H37Rv genome**

643 The regions most commonly excluded from *Mtb* genomics analysis, also referred to as the Putative  
644 Low Confidence (PLC) regions in this work, were based on current literature<sup>16,24,55,56</sup>. Specifically,  
645 we defined the PLC regions as the union of the 168 PE/PPE genes, all mobile genetic elements  
646 (MGEs), and 82 genes with repetitive content previously identified<sup>24</sup>. PLC regions are defined in  
647 **Additional File 19** (BED format). Non-PLC regions were simply defined as the complement of the  
648 PLC genes.

649

## 650 **Evaluating variant calling performance of genome masking approaches**

651 Following the small variant benchmarking standards outlined by the GA4GH, we used Hap.py  
652 (v0.3.13) to evaluate the Illumina WGS variant calling performance of Pilon for all 36 isolates  
653 individually. For each complete genome assembly, SNSs and small INDELs 1-15 bp inferred by the  
654 Minimap2-pattools pipeline were used as ground truth. We evaluated variant calling performance  
655 of Illumina WGS when using different region filtering schemas: (1) masking of all PLC genes, the

656 current standard practice, (2) masking of repetitive regions with P-Map-K50E4 < 100%, and (3) No  
657 masking. Masking schemas (1 and 2) are provided in BED format (**Additional File 19 and 20**).  
658 After applying each masking schema, we filtered potential variants according to whether the Pilon  
659 variant calling pipeline gave the variant a PASS filter and the mean mapping quality (MQ) of all  
660 reads aligned to the variant position.

661  
662 For each combination of region masking and variant filtering using mapping quality, we then  
663 calculated the absolute number of true positives (TP, i.e. a variant in the ground truth variant set  
664 and correctly called by the Illumina variant calling pipeline), false positives (FP, the Illumina variant  
665 calling pipeline calls a variant not in the ground truth set), and false negative (FN, the variant is in  
666 the ground truth set but is not called by the Illumina variant calling pipeline) variant calls. For each  
667 set of parameters, we calculated the overall precision (positive predictive value) as TP/(TP + FP),  
668 and recall (sensitivity) as TP/(TP + FN). In agreement with the default behavior of Hap.py, and to  
669 avoid undefined precision values, filtering parameters that yielded no TP or FP were defined as  
670 having a precision of 1.0 and a recall of 0. Additionally, we calculated the F1-score, which weights  
671 precision and recall with equally:  $F1 = 2 * (\text{precision} * \text{recall}) / (\text{precision} + \text{recall})$ . The F1 score  
672 summarizes each variant calling performance as a single value between 0 and 1 (where 1  
673 represents both perfect precision and recall).

674  
675 To aggregate the performance evaluation across all 36 isolates, the mean and standard error of  
676 the mean (SEM) of precision, recall and F1 score was calculated for all sets of parameters evaluated  
677 (**Additional File 10**). The individual variant calling performance statistics for each isolate can also  
678 be found in **Additional File 10**. The variant calling performance comparison of shorter (1-5bp) vs  
679 longer (6-15bp) INDELs can be found in **Additional File 11**.

680  
681 **Evaluating variant calling performance near regions with structural variation and**  
682 **repetitive sequence content**

683 Using Hap.py and the same approach defined in the above section, we evaluated SNS variant  
684 calling performance in the following types of regions: (1) SNSs in regions with perfect mappability  
685 (Pmap-K50E4 = 1) with no identified SV (2) SNSs in regions with low mappability (Pmap-K50E4 <  
686 1) with no identified SV, (3) SNSs in regions with perfect mappability within 100 bp of any  
687 identified SV, and (4) SNSs in regions with low mappability within 100bp of any identified SV.  
688 Genomic contexts not near SVs (1 and 2) were evaluated with MQ thresholds ranging from 1-60.  
689 For genomic contexts within 100 bp of an SV (3 and 4), the MQ thresholds evaluated ranged from  
690 1-40. The MQ threshold evaluated near SVs was limited due to the fact that a majority of SNSs  
691 near SVs typically have lower MQ values, and higher MQ values resulted in recalls of approximately  
692 0. As explained in the previous section, the mean and SEM of precision, recall, and F1 score were  
693 calculated for all MQ filtering thresholds across all 4 region types (**Additional File 12**).

694

695 **Evaluation of the distribution of potential false positive SNS calls across the Mtb**  
696 **genome**

697 False positive SNS calls were identified by the Hap.py evaluation software through comparison to  
698 the assembly-based ground truth variant call set. Additionally, false positive calls with  $MQ < 30$   
699 were filtered out, as to only include false positives which would realistically pass standard filtering.  
700 For each genomic region (gene or intergenic region) of the H37Rv genome, the total number of  
701 overlapping false positives across all 36 isolates was calculated (**Additional File 9**). Across all 36  
702 clinical isolates, there were 548 false positive SNSs with  $MQ \geq 30$  and 696 total false positive SNS  
703 with  $MQ \geq 1$  detected.

704

705 **Defining Refined Low Confidence (RLC) regions**

706 We defined the refined low confidence regions (RLC) of the Mtb reference genome as the union  
707 of A) The 30 false positive hot spot regions (gene and intergenic) identified (65 kb), B) poorly  
708 recalled genomic regions as identified by EBR (EBR  $< 0.9$ , 142 kb), and C) regions with frequently  
709 ambiguously defined ground truths (16 kb). We provide the complete set of RLC regions in BED  
710 format (177 kb, **Additional File 13**), along with each separate component of the RLC regions in  
711 BED format (**Additional Files 21, 22, and 23**). For very conservative masking of the Mtb reference  
712 genome, we additionally provide a masking scheme that specifies the union of a) the RLC regions  
713 and b) all low pileup mappability regions ( $PmapK50E4 < 1$ ) (277 kb, **Additional File 14**).

714

715

716

717

718

719

720

721

722

723

724

725

726

727

728

## 729 References

- 730 1. Li, H., Ruan, J. & Durbin, R. Mapping short DNA sequencing reads and calling variants using  
731 mapping quality scores. *Genome Res.* **18**, 1851–1858 (2008).
- 732 2. Li, H. Toward better understanding of artifacts in variant calling from high-coverage  
733 samples. *Bioinformatics* **30**, 2843–2851 (2014).
- 734 3. Nakamura, K. *et al.* Sequence-specific error profile of Illumina sequencers. *Nucleic Acids Res.*  
735 **39**, e90 (2011).
- 736 4. Ross, M. G. *et al.* Characterizing and measuring bias in sequence data. *Genome Biol.* **14**, R51  
737 (2013).
- 738 5. Goig, G. A., Blanco, S., Garcia-Basteiro, A. L. & Comas, I. Contaminant DNA in bacterial  
739 sequencing experiments is a major source of false genetic variability. *BMC Biol.* **18**, 24  
740 (2020).
- 741 6. Barbitoff, Y. A. *et al.* Systematic dissection of biases in whole-exome and whole-genome  
742 sequencing reveals major determinants of coding sequence coverage. *Sci. Rep.* **10**, 2057  
743 (2020).
- 744 7. Modlin, S. J. *et al.* Exact mapping of Illumina blind spots in the *Mycobacterium tuberculosis*  
745 genome reveals platform-wide and workflow-specific biases. *Microb Genom* (2021)  
746 doi:10.1099/mgen.0.000465.
- 747 8. Benjamini, Y. & Speed, T. P. Summarizing and correcting the GC content bias in high-  
748 throughput sequencing. *Nucleic Acids Res.* **40**, e72 (2012).
- 749 9. Aird, D. *et al.* Analyzing and minimizing PCR amplification bias in Illumina sequencing  
750 libraries. *Genome Biol.* **12**, R18 (2011).
- 751 10. Paten, B., Novak, A. M., Eizenga, J. M. & Garrison, E. Genome graphs and the evolution of  
752 genome inference. *Genome Res.* **27**, 665–676 (2017).
- 753 11. Garrison, E. *et al.* Variation graph toolkit improves read mapping by representing genetic  
754 variation in the reference. *Nat. Biotechnol.* **36**, 875–879 (2018).
- 755 12. Schmid, M. *et al.* Pushing the limits of de novo genome assembly for complex prokaryotic  
756 genomes harboring very long, near identical repeats. *Nucleic Acids Res.* **46**, 8953–8965  
757 (2018).
- 758 13. Rhoads, A. & Au, K. F. PacBio Sequencing and Its Applications. *Genomics Proteomics  
759 Bioinformatics* **13**, 278–289 (2015).
- 760 14. Wenger, A. M. *et al.* Accurate circular consensus long-read sequencing improves variant  
761 detection and assembly of a human genome. *Nat. Biotechnol.* **37**, 1155–1162 (2019).
- 762 15. De Maio, N. *et al.* Comparison of long-read sequencing technologies in the hybrid assembly  
763 of complex bacterial genomes. *Microb Genom* **5**, (2019).
- 764 16. Meehan, C. J. *et al.* Whole genome sequencing of *Mycobacterium tuberculosis*: current  
765 standards and open issues. *Nat. Rev. Microbiol.* (2019) doi:10.1038/s41579-019-0214-5.

766 17. Coscolla, M. & Gagneux, S. Consequences of genomic diversity in *Mycobacterium*  
767 *tuberculosis*. *Semin. Immunol.* **26**, 431–444 (2014).

768 18. Hicks, N. D. *et al.* Clinically prevalent mutations in *Mycobacterium tuberculosis* alter  
769 propionate metabolism and mediate multidrug tolerance. *Nat Microbiol* **3**, 1032–1042  
770 (2018).

771 19. Holt, K. E. *et al.* Frequent transmission of the *Mycobacterium tuberculosis* Beijing lineage  
772 and positive selection for the EsxW Beijing variant in Vietnam. *Nat. Genet.* **50**, 849–856  
773 (2018).

774 20. Chiner-Oms, Á. *et al.* Genome-wide mutational biases fuel transcriptional diversity in the  
775 *Mycobacterium tuberculosis* complex. *Nat. Commun.* **10**, 3994 (2019).

776 21. Ngabonziza, J. C. S. *et al.* A sister lineage of the *Mycobacterium tuberculosis* complex  
777 discovered in the African Great Lakes region. *Nat. Commun.* **11**, 2917 (2020).

778 22. Walker, B. J. *et al.* Pilon: an integrated tool for comprehensive microbial variant detection  
779 and genome assembly improvement. *PLoS One* **9**, e112963 (2014).

780 23. Krusche, P. *et al.* Best practices for benchmarking germline small-variant calls in human  
781 genomes. *Nat. Biotechnol.* **37**, 555–560 (2019).

782 24. Coscolla, M. *et al.* *M. tuberculosis* T Cell Epitope Analysis Reveals Paucity of Antigenic  
783 Variation and Identifies Rare Variable TB Antigens. *Cell Host Microbe* **18**, 538–548 (2015).

784 25. Thomas, S. K. *et al.* Modern and ancestral genotypes of *Mycobacterium tuberculosis* from  
785 Andhra Pradesh, India. *PLoS One* **6**, e27584 (2011).

786 26. Sharifpour, E., Farnia, P., Mozafari, M., Irani, S. & Akbar Velayati, A. Deletion of region of  
787 difference 181 in *Mycobacterium tuberculosis* Beijing strains. *Int J Mycobacteriol* **5 Suppl 1**,  
788 S238–S239 (2016).

789 27. Walter, K. S. *et al.* Genomic variant-identification methods may alter *Mycobacterium*  
790 *tuberculosis* transmission inferences. *Microb Genom* **6**, (2020).

791 28. Jajou, R. *et al.* Towards standardisation: comparison of five whole genome sequencing  
792 (WGS) analysis pipelines for detection of epidemiologically linked tuberculosis cases. *Euro  
793 Surveill.* **24**, (2019).

794 29. Farhat, M. R. *et al.* GWAS for quantitative resistance phenotypes in *Mycobacterium*  
795 *tuberculosis* reveals resistance genes and regulatory regions. *Nat. Commun.* **10**, 2128  
796 (2019).

797 30. Rosenthal, A. *et al.* The TB Portals: an Open-Access, Web-Based Platform for Global Drug-  
798 Resistant-Tuberculosis Data Sharing and Analysis. *J. Clin. Microbiol.* **55**, 3267–3282 (2017).

799 31. Epperson, L. E. & Strong, M. A scalable, efficient, and safe method to prepare high quality  
800 DNA from mycobacteria and other challenging cells. *J Clin Tuberc Other Mycobact Dis* **19**,  
801 100150 (2020).

802 32. Wilson, K. Preparation of genomic DNA from bacteria. *Curr. Protoc. Mol. Biol.* **Chapter 2**,  
803 Unit 2.4 (2001).

804 33. Kapopoulou, A., Lew, J. M. & Cole, S. T. The MycoBrowser portal: a comprehensive and  
805 manually annotated resource for mycobacterial genomes. *Tuberculosis* **91**, 8–13 (2011).

806 34. Ates, L. S. New insights into the mycobacterial PE and PPE proteins provide a framework for  
807 future research. *Mol. Microbiol.* (2019) doi:10.1111/mmi.14409.

808 35. Zulkower, V. & Rosser, S. DNA Features Viewer: a sequence annotation formatting and  
809 plotting library for Python. *Bioinformatics* **36**, 4350–4352 (2020).

810 36. Kolmogorov, M., Yuan, J., Lin, Y. & Pevzner, P. A. Assembly of long, error-prone reads using  
811 repeat graphs. *Nat. Biotechnol.* **37**, 540–546 (2019).

812 37. Hunt, M. *et al.* Circlator: automated circularization of genome assemblies using long  
813 sequencing reads. *Genome Biol.* **16**, 294 (2015).

814 38. Bolger, A. M., Lohse, M. & Usadel, B. Trimmomatic: a flexible trimmer for Illumina sequence  
815 data. *Bioinformatics* **30**, 2114–2120 (2014).

816 39. Li, H. Aligning sequence reads, clone sequences and assembly contigs with BWA-MEM.  
817 *arXiv [q-bio.GN]* (2013).

818 40. Picard Tools - By Broad Institute. <http://broadinstitute.github.io/picard/>.

819 41. Wyllie, D. H. *et al.* Identifying Mixed Mycobacterium tuberculosis Infection and Laboratory  
820 Cross-Contamination during Mycobacterial Sequencing Programs. *J. Clin. Microbiol.* **56**,  
821 (2018).

822 42. Jain, C., Rodriguez-R, L. M., Phillippy, A. M., Konstantinidis, K. T. & Aluru, S. High throughput  
823 ANI analysis of 90K prokaryotic genomes reveals clear species boundaries. *Nat. Commun.* **9**,  
824 5114 (2018).

825 43. Seemann, T. Prokka: rapid prokaryotic genome annotation. *Bioinformatics* **30**, 2068–2069  
826 (2014).

827 44. Darling, A. E., Mau, B. & Perna, N. T. progressiveMauve: multiple genome alignment with  
828 gene gain, loss and rearrangement. *PLoS One* **5**, e11147 (2010).

829 45. Darling, A. C. E., Mau, B., Blattner, F. R. & Perna, N. T. Mauve: multiple alignment of  
830 conserved genomic sequence with rearrangements. *Genome Res.* **14**, 1394–1403 (2004).

831 46. Li, H. Minimap2: pairwise alignment for nucleotide sequences. *Bioinformatics* **34**, 3094–3100  
832 (2018).

833 47. Khelik, K., Lagesen, K., Sandve, G. K., Rognes, T. & Nederbragt, A. J. NucDiff: in-depth  
834 characterization and annotation of differences between two sets of DNA sequences. *BMC  
835 Bioinformatics* **18**, 338 (2017).

836 48. Kurtz, S. *et al.* Versatile and open software for comparing large genomes. *Genome Biol.* **5**,  
837 R12 (2004).

838 49. Danecek, P. *et al.* Twelve years of SAMtools and BCFtools. *Gigascience* **10**, (2021).

839 50. Li, H. A statistical framework for SNP calling, mutation discovery, association mapping and  
840 population genetical parameter estimation from sequencing data. *Bioinformatics* **27**, 2987–  
841 2993 (2011).

842 51. Quinlan, A. R. & Hall, I. M. BEDTools: a flexible suite of utilities for comparing genomic  
843 features. *Bioinformatics* **26**, 841–842 (2010).

844 52. Price, M. N., Dehal, P. S. & Arkin, A. P. FastTree 2--approximately maximum-likelihood trees  
845 for large alignments. *PLoS One* **5**, e9490 (2010).

846 53. Derrien, T. *et al.* Fast computation and applications of genome mappability. *PLoS One* **7**,  
847 e30377 (2012).

848 54. Pockrandt, C., Alzamel, M., Iliopoulos, C. S. & Reinert, K. GenMap: Ultra-fast Computation of  
849 Genome Mappability. *Bioinformatics* (2020) doi:10.1093/bioinformatics/btaa222.

850 55. Lee, R. S., Proulx, J.-F., McIntosh, F., Behr, M. A. & Hanage, W. P. Previously undetected  
851 super-spreading of *Mycobacterium tuberculosis* revealed by deep sequencing. *Elife* **9**,  
852 e53245 (2020).

853 56. Coscolla, M. *et al.* Phylogenomics of *Mycobacterium africanum* reveals a new lineage and a  
854 complex evolutionary history. *Microb Genom* (2021) doi:10.1099/mgen.0.000477.

855 57. Borrell, S. *et al.* Reference set of *Mycobacterium tuberculosis* clinical strains: A tool for  
856 research and product development. *PLoS One* **14**, e0214088 (2019).

857 58. Köster, J. & Rahmann, S. Snakemake--a scalable bioinformatics workflow engine.  
858 *Bioinformatics* **28**, 2520–2522 (2012).

859 59. Marin, M. G. *Additional File 6 - Base level analysis of Empirical Base Pair Recall, Pileup*  
860 *Mappability, and GC content across the H37Rv genome.* (2021). doi:10.5281/zenodo.4662193.

861

862

## 863 **Author Contributions**

864 MGM and MRF conceived, designed and conducted the study. MGM and MRF wrote the  
865 manuscript with input from all authors. RVJ provided bioinformatics support and input on data  
866 analysis. LEE, DD, M. Salfinger and M. Strong cultured Mtb isolates and performed DNA extraction  
867 in preparation for PacBio sequencing of Dataset #1. IA, SV, and VC cultured Mtb isolates and  
868 performed DNA extraction in preparation for PacBio sequencing of Dataset #2.. AR, MH, and BJ  
869 selected clinical isolates and assisted in data processing for PacBio sequencing of Dataset #2. ZI  
870 provided help and advice throughout the project. The final manuscript was read and approved by  
871 all authors.

## 872 **Competing Interests**

873 The authors declare that they have no competing interests.

## 874 **Data availability and materials**

875 All new sequencing data generated for this study and complete *Mtb* genome assemblies were  
876 submitted to NCBI SRA and Genbank databases under BioProject accession number PRJNA719670  
877 (Submission Pending). The publicly available PacBio and Illumina data from two previously  
878 published studies<sup>20,21,57</sup> is available from PRJEB8783, PRJEB31443, PRJEB27802, and PRJNA598991.  
879 SRA/ENA accessions and related sequencing metadata for all data can be found in Additional File  
880 15. All code for data processing and analysis in this study is available from the following GitHub  
881 repository, <https://github.com/farhat-lab/mtb-illumina-wgs-evaluation>. The repository README  
882 provides instructions to run each part of the analysis using the Snakemake<sup>58</sup> workflow engine and  
883 using Python based Jupyter notebooks.

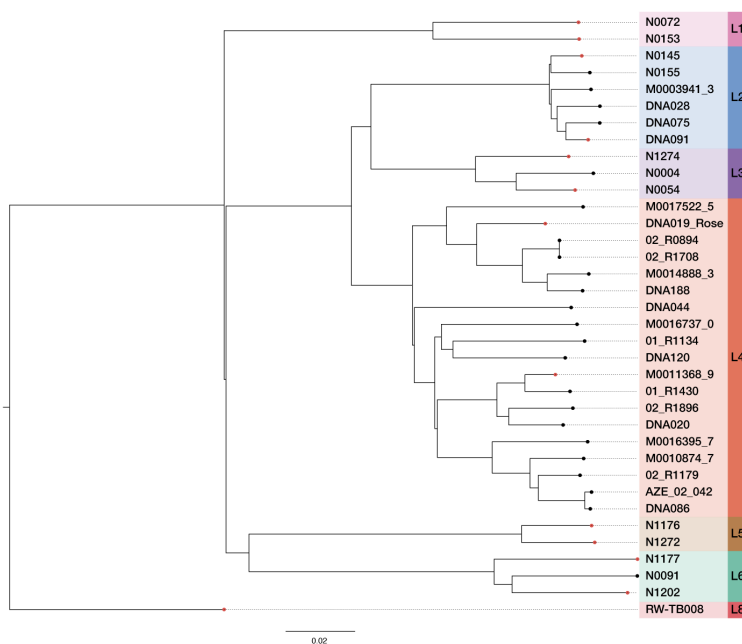
## 884 **Acknowledgments**

885 We are grateful to Natalia Quiñones, and Karel Brinda for their helpful discussions and advise  
886 throughout the project. We grateful to Melissa Smith and Irina Oussenko for their assistance in  
887 PacBio (RS II) long read sequencing of the *M. tuberculosis* genomic DNA. We acknowledge NIH  
888 Intramural Sequencing Center (NISC) for the PacBio (Sequel II) long-read sequencing of the *M.*  
889 *tuberculosis* genomic DNA; Critical Path Institute (C-Path) and Translational Genomics Research  
890 Institute (T-Gen) for the Illumina sequencing of the *M. tuberculosis* DNAs and for the mTB DNA  
891 long-term storage; the International Science and Technology Center for their support in  
892 establishing the TB Portal agreement with Georgia; CRDF Global for their support in establishing  
893 the TB Portal agreements with Azerbaijan and Moldova. This research was supported in part by  
894 the Office of Science Management and Operations of the NIAID.  
895  
896  
897  
898  
899  
900  
901  
902  
903  
904  
905  
906  
907  
908  
909

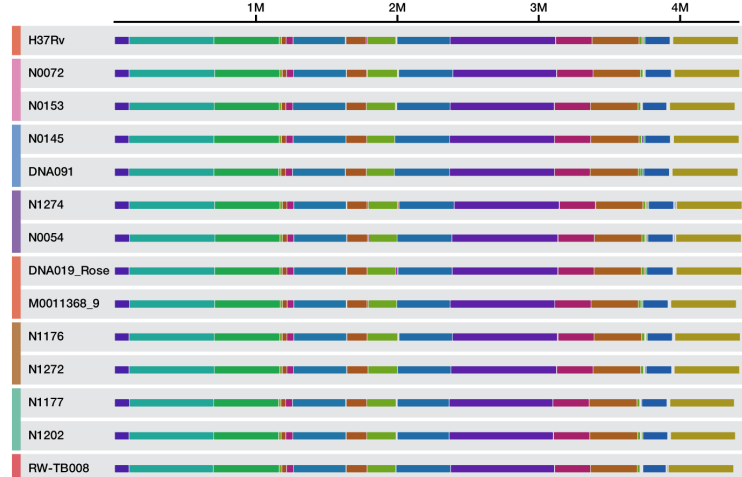
910 **Figures & Tables**

911 **Figure 1**

A



B



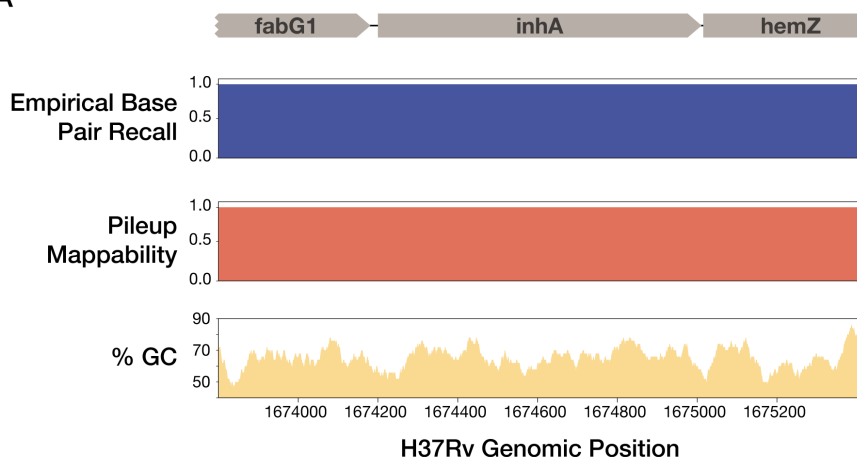
912

913 **Overview of 36 clinical *Mtb* isolates with completed genome assemblies. a)** Maximum  
914 likelihood Phylogeny of *M. tuberculosis* isolates with PacBio complete genome assemblies. The  
915 sequences of all 36 complete *M. tb* genomes were aligned to the H37rv reference genome using  
916 minimap2, and a maximum likelihood phylogeny was inferred using a concatenated SNS alignment  
917 (15,673 total positions). **b)** Representative isolates from each lineage sampled from the whole  
918 genome sequence alignment between the H37Rv reference genome and all completed circular  
919 *Mtb* genome assemblies, The complete alignment is visualized in Supplemental Figure 2. The  
920 whole genome multiple sequence alignment was performed using the *progressiveMauve*<sup>44</sup>  
921 algorithm. Each contiguously colored region is a locally collinear block (LCB), a region without  
922 rearrangement of homologous backbone sequence.

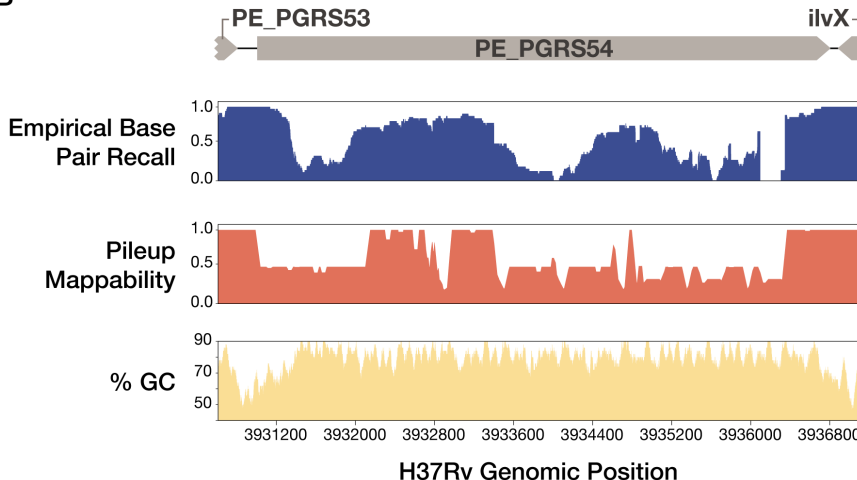
923

924 **Figure 2**

A



B



925

926

**EBR, Pileup Mappability, and GC content across two example regions of the H37Rv genome.**

927

Empirical Base Pair Recall (EBR), Pileup Mappability (K=50 bp, e = 4 mismatches) and GC% (100 bp window) values are plotted across all base pair positions of two regions of interest. **a)** *InhA*, an antibiotic resistance gene, shows perfect EBR across the entire gene body. **b)** In contrast, *PE\_PGRS54*, a known highly repetitive gene with high GC content, has extremely low EBR across the entire gene body. Browser tracks of EBR and Pileup Mappability in BEDGRAPH format are made available as Additional Files 17 and 18.

931

932

933

934

935

936

937

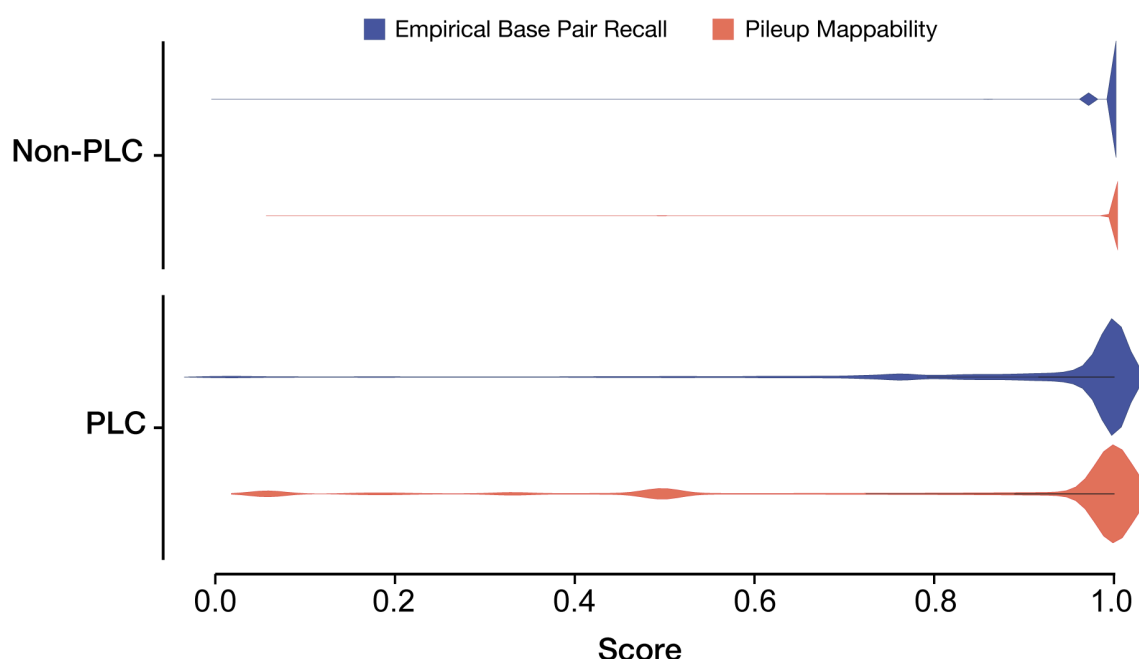
938

939

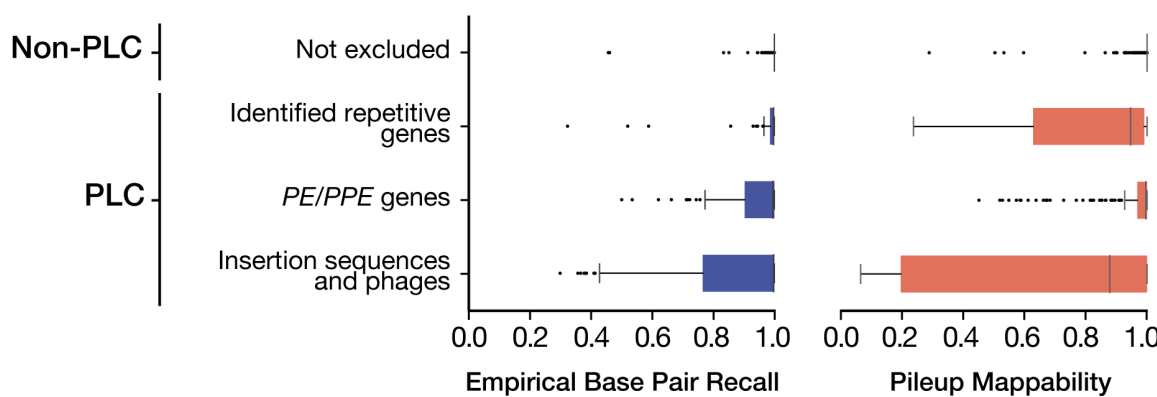
940

941 **Figure 3**

A



B



942

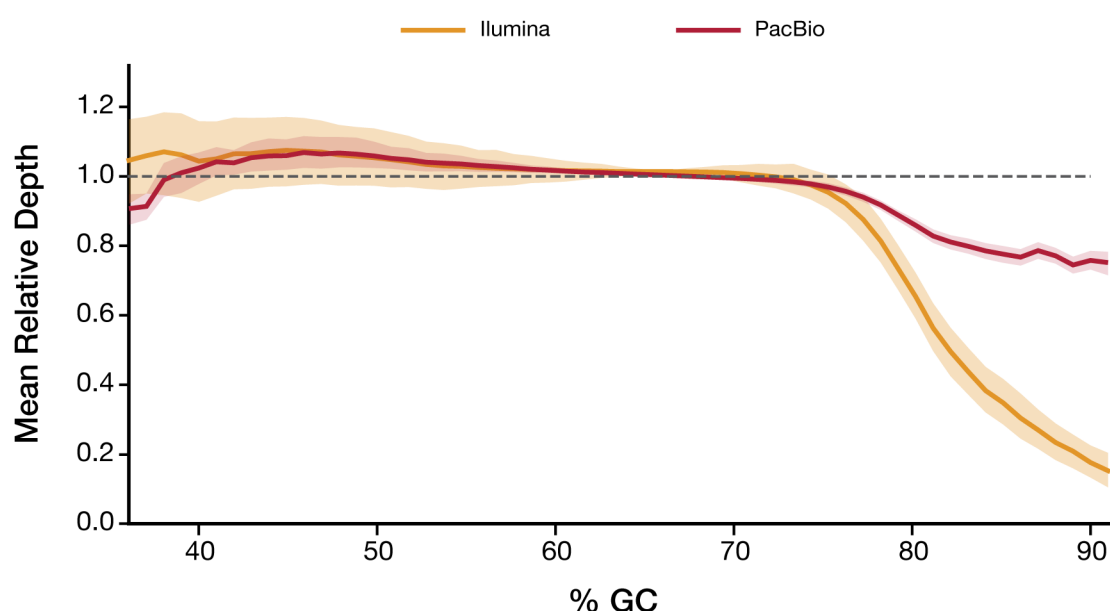
943 **The Distribution of EBR and Pileup Mappability scores in PLC and non-PLC regions. a)** The distribution of  
944 Empirical Base Pair Recall (EBR) and Pileup Mappability (P-Map,  $K=50, E=4$ ) scores of PLC and non-PLC regions.  
945 Excluded regions harbor significantly more low EBR base pair positions when compared to the included genes,  
946 but 68% of routinely excluded positions still have  $\geq 97\%$  EBR. The Pileup mappability with  $K=50$  bp is lower in  
947 PLC regions (mean = 0.86) than non-PLC regions (mean = .997). **b)** The Distribution of gene-level mean EBR  
948 and P-Map ( $K=50, E=4$ ) between PLC and non-PLC regions. We compared the mean EBR and Pileup  
949 Mappability across all genes within PLC and non-PLC regions. The pe and ppe gene families (PE/PPEs) and  
950 mobile genetic elements (MGE), which make up 82% of PLC genes, demonstrated significantly lower mean EBR  
951 and Pileup Mappability than other non-PLC genes.  
952

953

954

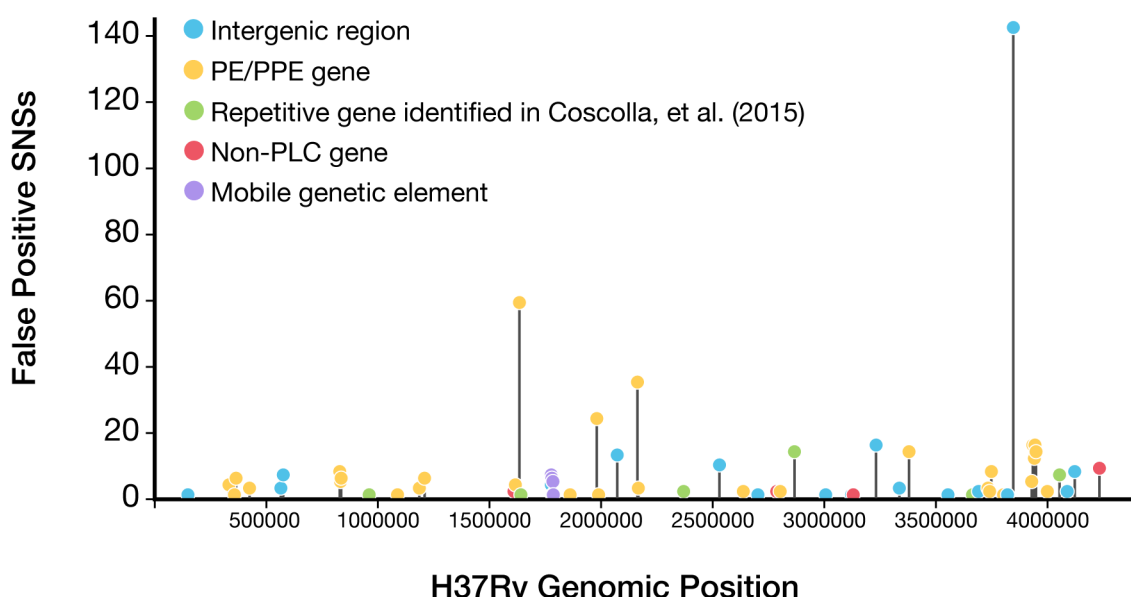
955

956 **Figure 4**



957  
958 **Relative sequencing depth as a function of local GC content across all 36 complete isolates.** We evaluated the  
959 relative depth of our Illumina and PacBio sequencing data as a function of GC content (100 bp window size) across all  
960 positions of each isolate's complete genome assembly. The relative depth was averaged across all positions with the  
961 same GC% across each genome assembly. The standard error of the mean of the relative depth across all 36 isolates is  
962 shaded for each sequencing technology. At high (>70%) GC contents, Illumina starts to show lower relative depth  
963 compared to PacBio sequencing.  
964  
965  
966  
967

968 **Figure 5**



969  
970 **The distribution of potential false positive SNS calls across all genomic regions of the H37Rv genome.** The  
971 frequency of false positive SNS calls detected ( $MQ \geq 30$ ) across all 36 isolates evaluated was plotted for all regions of  
972 the H37Rv genome (gene or intergenic regions). The top 30 regions ranked by the number of total false positives  
973 contained 89.4% (490/548) of the total false positive SNSs and spanned only 65 kb of the H37Rv genome. Full results  
974 for all annotated genomic regions (gene or intergenic) can be found in Additional File 9.

975

976

977

978

979

980

981

982

983

984

985

986

987

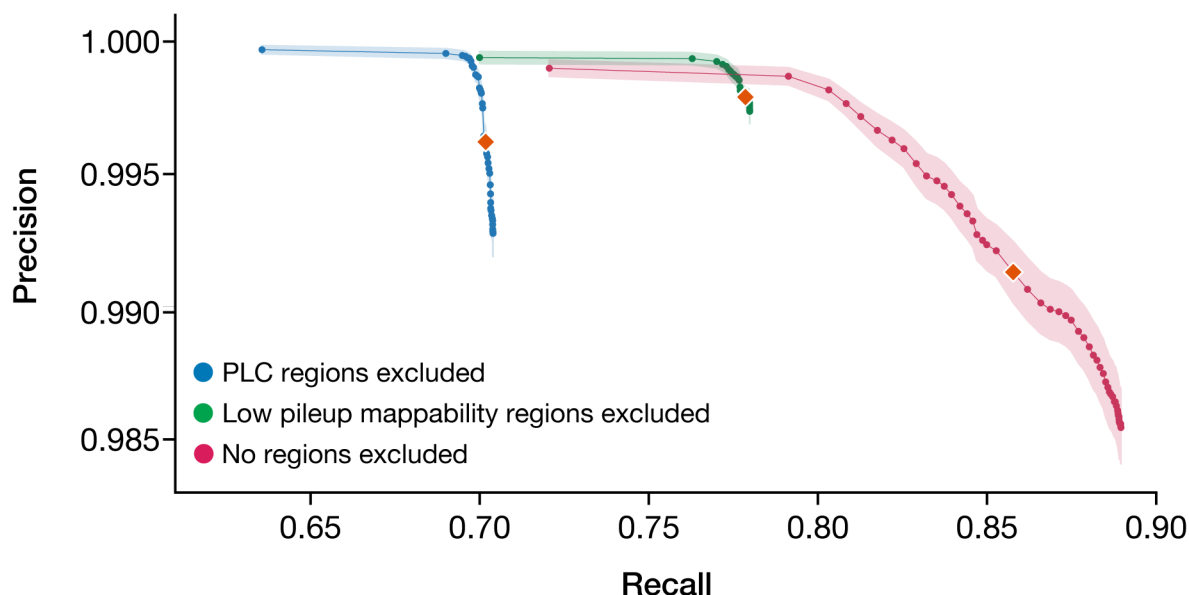
988

989

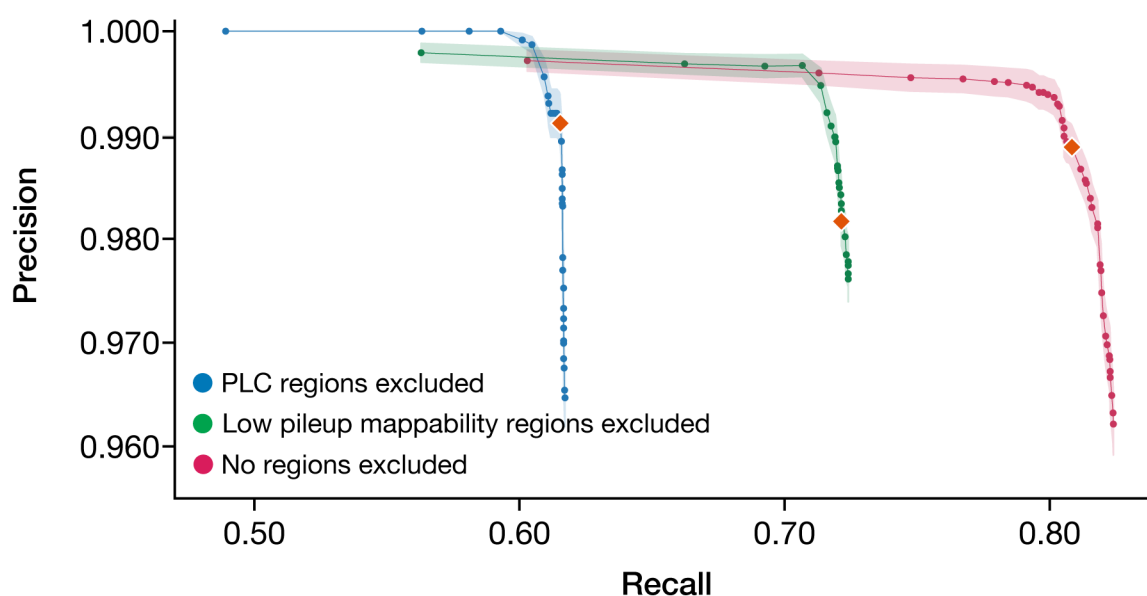
990

991 **Figure 6**

A



B



992

993

994

995

996

997

998

999

1000

**Mean SNV and INDEL variant calling performance across different masking approaches. a)** SNS variant calling performance was evaluated across the following three schemas: (1) masking of regions with non-unique sequence, as defined as positions with P-Map-K50E4 < 1, (2) No *a priori* masking of any regions, and compared to (3) masking of all PLC genes (the current standard practice). **(b)** short INDEL (1-15 bp) variant calling performance was evaluated across the same schemas. The orange diamonds represent the mean precision and recall using a MQ threshold of 40 for both (a) and (b). Shaded regions represent the SEM of precision across all 36 isolates evaluated. For all masking approaches evaluated, the MQ thresholds evaluated ranged from 1-60. Complete benchmarking results can be found for each individual isolate in Additional File 10.

1001

**Table 1.**

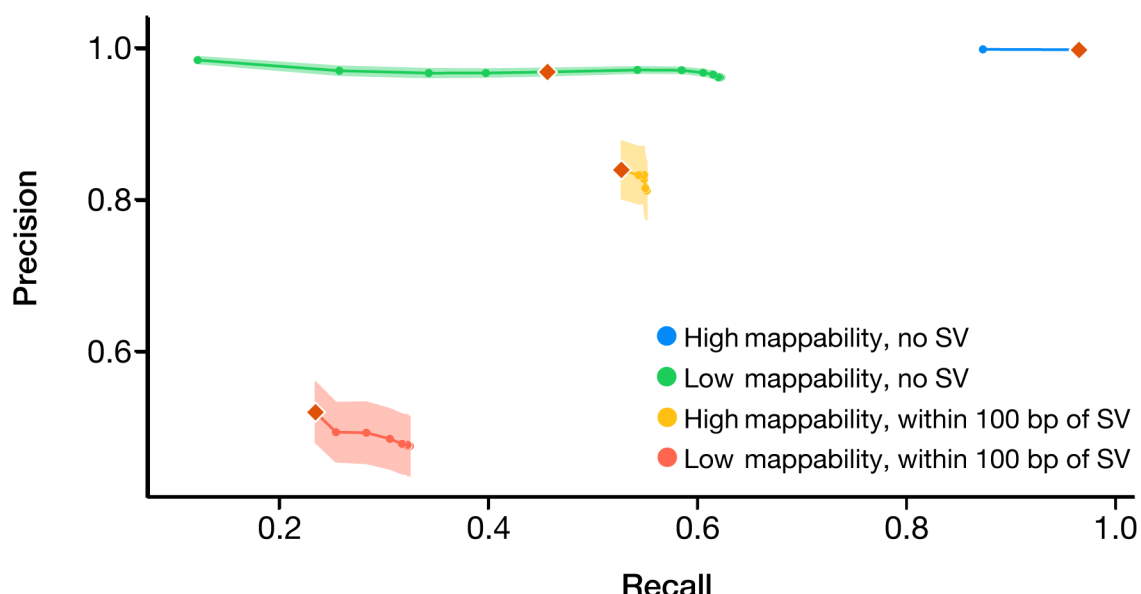
<b>Masking Schema</b>	<b>Metric Optimized</b>	<b>MQ Threshold</b>	<b>F1</b>	<b>Precision</b>	<b>Recall</b>
Masking non-unique regions	F1-score	19	0.87	99.77%	77.98%
	Comparator	40	0.88	99.79%	77.86%
	Precision	60	0.82	99.94%	70.00%
No masking	F1-score	8	0.94	98.56%	88.95%
	Comparator	40	0.92	99.13%	85.77%
	Precision	60	0.83	99.90%	72.06%
Masking PLC genes (current standard)	F1-score	35	0.82	99.50%	70.30%
	Comparator	40	0.82	99.62%	70.17%
	Precision	60	0.77	99.97%	63.56%

1002  
1003  
1004  
1005

**Comparison of performance of proposed genome-masking schemas for SNS variant calling.** For each masking scheme and MQ filtering threshold shown, the corresponding mean Precision, Recall, and F1 score is shown across all 36 *Mtb* isolates. Corresponding Precision-Recall curves are given in Figure 5A. Performance at a threshold of  $\text{MQ} \geq 40$  is given as a common point of comparison across the three masking schemas.

1006  
1007  
1008  
1009  
1010  
1011  
1012  
1013  
1014  
1015  
1016  
1017  
1018  
1019  
1020  
1021

1022 **Figure 7**



1023  
1024 **Variant calling performance of single nucleotide substitutions stratified by proximity to structural variants**  
1025 **and low pileup mappability sequence.** Mappability is dichotomized at Pmap-K50E4 =100% or <100%. Regions  
1026 within 100bp of a SV categorized as "with SV". Precision and recall is plotted for the following genomic contexts: (1)  
1027 regions with high mappability with no SV (Blue, F1 = 0.98 (precision = 99.89%, recall = 96.49%, MQ threshold of 40)),  
1028 (2) regions with low mappability and no SV (green, F1 = 0.62 (precision = 96.98%, recall = 45.65%, MQ threshold of  
1029 40), (3) regions with high mappability with SV (orange, F1 = 0.64 (precision = 84.07%, recall = 52.73%, MQ threshold  
1030 of 40), (4) regions with low mappability and with SV (red, F1 = 0.32 (precision = 52.10%, recall = 23.47%, MQ  
1031 threshold of 40). The standard error of the mean (SEM) for precision is shaded for each curve. Orange diamonds  
1032 represent the precision and recall using the same MQ threshold of 40. Genomic contexts not near SVs (1 and 2) were  
1033 evaluated with MQ thresholds ranging from 1-60. For genomic contexts within 100 bp of an SV (3 and 4), the MQ  
1034 thresholds evaluated ranged from 1-40. Complete benchmarking results can be found for each individual isolate in  
1035 Additional File 12.

## 1048 **Supplementary Information**

1049 Additional File 1: Supplementary Figures and Tables (Figure S1-7, Table S1-6)

1050

1051 Additional File 2: Results and quality control for assembly and sequencing for both PacBio and Illumina

1052 sequencing

1053

1054 Additional File 3: List of all changes made during Illumina polishing of the *de novo* PacBio assemblies

1055

1056 Additional File 4: List of genomic regions with ambiguously defined ground truths relative to H37Rv for all

1057 each isolate evaluation

1058

1059 Additional File 5: List of genomic regions which were frequently had an ambiguously defined ground truth

1060

1061 Additional File 6: Table containing the EBR, Pileup Mappability, and GC% of all genomic positions of the

1062 H37Rv reference. Due to large file size, Additional File 6<sup>59</sup> is hosted on Zenodo at

1063 <https://zenodo.org/record/4662193>.

1064

1065 Additional File 7: EBR, and Pileup Mappability across all genomic regions of H37Rv (both genes and

1066 intergenic regions)

1067

1068 Additional File 8: Table of the mean relative sequencing depth of both Illumina and PacBio at varying GC%

1069 across all 36 isolates evaluated.

1070

1071 Additional File 9: Table containing the frequency of observed False Positive SNSs (MQ  $\geq$  30) across all

1072 genomic regions of H37Rv (both genes and intergenic regions)

1073

1074 Additional File 10: Variant call benchmarking of SNSs and small indels (<=15bp)

1075

1076 Additional File 11: Variant call benchmarking stratified by shorter (< 6bp) and longer indels (6-15bp)

1077

1078 Additional File 12: Variant call benchmarking of SNSs stratified by proximity to an SV and low pileup

1079 mappability

1080

1081 Additional File 13: Masking scheme in BED format specifying the Refined Low Confidence Regions

1082

1083 Additional File 14: Masking scheme in BED format specifying the union of a) Refined Low Confidence

1084 Regions, and b) regions with Pileup Mappability (K= 50 bp, E = 4 mismatches) < 1.

1085

1086

1087

1088

1089

1090 Additional File 15: SRA/ENA sequencing run metadata for PacBio and Illumina sequencing used in this  
1091 study  
1092  
1093 Additional File 16: All identified structural variants for each complete genome assembly as identified by  
1094 the NucDiff analysis pipeline.  
1095  
1096 Additional File 17: Base-level Pileup Mappability scores (P-Map-K50E4) across the H37Rv in BEDGRAPH  
1097 format  
1098  
1099 Additional File 18: Base-level EBR scores (36 isolates) across the H37Rv in BEDGRAPH format  
1100  
1101 Additional File 19: Masking scheme for the Putative Low Confidence (PLC) Regions in BED format  
1102  
1103 Additional File 20: All regions with low pileup mappability (P-Map-K50E4 < 100%) in BED format  
1104  
1105 Additional File 21: Component (A) of RLC regions. Masking scheme Specifying the 30 false positive hot  
1106 spot regions (gene and intergenic) in BED format.  
1107  
1108 Additional File 22:  
1109 Component (B) of RLC regions. Masking scheme specifying poorly recalled genomic regions as identified  
1110 by EBR< 0.9) in BED format.  
1111  
1112 Additional File 23:  
1113 Component (C) of RLC regions. Masking scheme specifying regions that frequently (> 25%) had an  
1114 ambiguously defined ground truth in BED format. Same information as Additional File 5 but this file is  
1115 instead in BED format.